Somali Jet Changes under the Global Warming*

LIN Meijing[1,2†](林美静), FAN Ke[1](范 可), and WANG Huijun[1](王会军)

1 *Nansen-Zhu International Research Center, Institute of Atmospheric Physics, Chinese Academy of Sciences, Beijing* 100029

2 *Graduate School of the Chinese Academy of Sciences, Beijing* 100039

(Received October 16, 2008)

ABSTRACT

Somali Jet changes will influence the variability of Asian monsoon and climate. How would Somali Jet changes respond to the global warming in the future climate? To address this question, we first evaluate the ability of IPCC-AR4 climate models and perform the 20th century climate in coupled models (20C3M) experiments to reproduce the observational features of the low level Somali Jet in JJA (June-July-August) for the period 1976–1999. Then, we project and discuss the changes of Somali Jet under the climate change of Scenario A2 (SRESA2) for the period 2005–2099. The results show that 18 IPCC-AR4 models have performed better in describing the climatological features of Somali Jet in the present climate simulations. Analysis of Somali Jet intensity changes from the multi-model ensemble results for the period 2005–2099 shows a weakened Somali Jet in the early 21st century (2010–2040), the strongest Somali Jet in the middle 21st century (2050–2060), as well as the weakest Somali Jet at the end of the 21st century (2070–2090). Compared with the period 1976–1999, the intensity of Somali Jet is weakening in general, and it becomes the weakest at the end of the 21st century. The results also suggest that the relationship between the intensity of Somali Jet in JJA and the increment of global mean surface air temperature is nonlinear, which is reflected differently among the models, suggesting the uncertainty of the IPCC-AR4 models. Considering the important role of Somali Jet in the Indian monsoon and East Asian monsoon and climate of China, the variability of Somali Jet and its evolvement under the present climate or future climate changes need to be further clarified.

Key words: IPCC-AR4 models, Somali Jet changes, global warming

1. Introduction

As an important component of Asian monsoon system, a strong cross-equatorial low level Somali Jet transports momentum and water vapor in inter-hemispheres. Recent results indicate Somali Jet transports water vapor from the winter to the summer hemisphere (Li et al., 2000; Wang and Xue, 2003; Shi et al., 2001; Li et al., 2004). The variability of Somali Jet on the intraseasonal, interannual, and decadal time scales will directly influence the East Asian summer monsoon rainfall (Li et al., 2006; Gao and Xue, 2006; Cong et al., 2007; Wang and Yang, 2008). It is found that when Somali Jet occurs more strongly in May-June than the multi-year average, the South China Sea summer monsoon will break out earlier than normal (Gao and Xue, 2006). The energy of Somali Jet will be dispersed northeastward, resulting in the anomalous East Asian climate. It is found that the interannual and decadal variabilities of Somali Jet are associated with the location of the West Pacific subtropical high, ENSO, and Pacific decadal oscillation (PDO) as well (Wang and Yang, 2008).

Projection of future changes of both Asian monsoon and regional climate under global warming has been a frontier topic. Simulation of the Somali Jet variability is also a major aspect of climate model validations. Some studies have been carried out along this direction (Wang et al., 1992; Zhao and Luo, 1998; Gao et al., 2003; Jiang et al., 2004; Zhou and Yu, 2006; Vera et al., 2006; Hori and Ueda, 2006; Xu et al., 2007; Jiang et al., 2008). However, future changes of Somali Jet under global warming have not been discussed so far. What the future changes of Somali Jet would be

*Supported by the Basic Research Development Program of China (973 Program) under Grant No. 2009CB421406, the Research Fund for excellent Ph. D dissertations in Chinese Academy of Sciences, and the National Natural Science Foundation of China under Grant No. 40523001.

†Corresoonding author: lmj@mail.iap.ac.cn.

under the global warming is an important issue. Basing on the IPCC-AR4 models outputs for the 20th century climate in coupled models (20C3M) and in the Scenario A2 (SRESA2) for the 21st century climate simulations, we analyze the changes of Somali Jet in the 21st century and investigate the relationship between the intensity of Somali Jet and increase of global mean surface temperature. Our results will help to provide the basis for the research of future changes of Asian monsoon and East Asian climate.

2. Data

The model data is obtained from the website: http://www-pcmdi.llnl.gov/projects/cmip/index.php. The outputs of 20C3M are used to describe the climate for the period 1976–1999, while those from the SRESA2 are used to represent future climate change for the period 2005–2099. Eighteen IPCC-AR4 models are denoted A-R, respectively. They are A: BCCRBCM2.0 (Norway), B: CGCM3.1(T47) (Canada), C: CNRM-CM3 (France), D:CSIRO-MK3.0 (Australia), E: CSIRO-MK3.5 (Australia), F: GFDL-CM2.0 (USA), G: GFDL-CM2.1 (USA), H: GISS-ER (USA), I: INGV-SXG (Italy), J: INM-CM3.0 (Russia), K: IPSL-CM4 (France), L: MIROC3.2 (medres) (Japan), M: ECHAM5/MPI-OM (Germany), N: MRI-CGCM2.3.2 (Japan), O: CCSM3 (USA), P: PCM (USA), Q: UKMO-HadCM3 (UK), and R: UKMO-HadGEM1 (UK). The details of the models are documented at the website above. In addition, relevant information about model evaluation and brief model introduction can also be found in Chapter 8 of the IPCC AR4 Working Group I Report, at the website: http://www.ipcc.ch/ipccreports/ar4-wg1.htm.

The initial fields for the models in 20C3M are from the preindustrial control (PICNTRL) experiment. The models are driven with external climate forcings such as anthropogenic increases in greenhouse gases and sulphate aerosols, changes in solar radiation and forcing by explosive volcanism; the different forcings are incorporated either into separate simulations or into one simulation (Hegerl et al., 2003). The concentration of greenhouse gases which changes with time is from observation or reconstruction of the history sequence. The initial fields for the models in SRESA2, which is a high greenhouse gas emission experiment, are from the multi-model ensemble results in year 1990 of Scenario 20C3M experiments. An introduction on the external forcings (including concentration of greenhouse gas, sulfate aerosols, solar radiation, and volcanic eruption) can be found at the website: http://www.ccsm.ucar.edu/working_groups/Change/CCSM3_IPCC_AR4/SRESA2.html and in Chapter 10 of the IPCC AR4 Working Group I Report.

The area of 20°S–30°N, 30–140°E is dominated by cross-equatorial flow (Li and Lou, 1987) and is selected as a key domain to evaluate the model performance in this paper. The Somali Jet index is defined as area-averaged wind velocity at 850 hPa in June-July-August (JJA) over the region 15°S–10°N, 37.5°–62.5°E (Wang and Xue, 2003).

The multi-model ensemble is obtained by averaging the outputs from the 18 models. The present climate period refers to 1976–1999, and the future climate period refers to 2005–2099. The observational datasets are derived from the NCEP/NCAR reanalysis and ERA-40 for the period 1976–1999. Summer mean denotes the average of JJA.

3. Simulated Somali Jet in the present climate

3.1 Simulated spatial distribution

In comparison with two observational datasets NCEP/NCAR reanalysis and ERA-40 for 1976–1999, simulated winds at 200 and 850 hPa in the region 20°S–30°N, 30°–140°E are analyzed. Table 1 shows the wind spatial correlation coefficients in the region 20°S–30°N, 30°–140°E between models and observations. Each model and the 18-model ensemble well reproduce the observational zonal wind at 200 and 850 hPa, with the zonal wind spatial correlation coefficients between 20C3M models and NCEP/NCAR (ERA-40) data about 0.9. As far as the meridional wind is concerned, the values of meridional wind spatial correlation coefficients between 20C3M models and NCEP/NCAR (ERA-40) data are in the range of 0.6–0.9, while the values of meridional wind spatial correlation coefficients between the 18-model ensemble and NCEP/NCAR (ERA-40) data are larger than

0.9. Table 1 illustrates that any model can simulate the observational spatial features, but the simulation ability for each model is different. The high values of wind correlation coefficients between the multi-model ensemble and NCEP/NCAR (ERA-40) data suggest that the multi-model ensemble could improve the capability to capture the basic features of winds in the region 20°S–30°N, 30°–140°E.

Table 1. Spatial correlation coefficients of wind over the area of 20°S–30°N, 30°–140°E between 20C3M models results and NCEP/NCAR and ERA-40 reanalysis

	(ERA40)U850	(ERA40)U200	(ERA40)V850	(ERA40)V200
18 mean	0.97(0.96)	0.98(0.99)	0.92(0.91)	0.93(0.94)
A	0.96(0.95)	0.96(0.96)	0.88(0.85)	0.80(0.83)
B	0.95(0.96)	0.93(0.94)	0.91(0.89)	0.90(0.89)
C	0.94(0.92)	0.97(0.96)	0.86(0.82)	0.81(0.82)
D	0.93(0.91)	0.96(0.97)	0.85(0.83)	0.93(0.92)
E	0.93(0.91)	0.96(0.97)	0.84(0.83)	0.90(0.89)
F	0.96(0.95)	0.97(0.98)	0.89(0.88)	0.90(0.91)
G	0.97(0.96)	0.98(0.98)	0.91(0.91)	0.94(0.93)
H	0.84(0.83)	0.97(0.96)	0.79(0.76)	0.69(0.67)
I	0.94(0.94)	0.97(0.96)	0.88(0.89)	0.89(0.89)
J	0.88(0.85)	0.96(0.94)	0.80(0.70)	0.81(0.79)
K	0.92(0.89)	0.87(0.86)	0.83(0.83)	0.84(0.80)
L	0.92(0.92)	0.98(0.98)	0.88(0.85)	0.85(0.87)
M	0.94(0.94)	0.96(0.97)	0.87(0.91)	0.88(0.88)
N	0.91(0.89)	0.90(0.92)	0.85(0.84)	0.83(0.84)
O	0.94(0.93)	0.96(0.97)	0.89(0.86)	0.87(0.87)
P	0.87(0.85)	0.89(0.90)	0.81(0.78)	0.73(0.72)
Q	0.95(0.95)	0.92(0.94)	0.80(0.84)	0.87(0.89)
R	0.95(0.95)	0.92(0.95)	0.83(0.86)	0.86(0.88)

Each correlation coefficient is at 99% significant level.

3.2 Simulated climatological features of Somali Jet

The multi-model ensemble is able to well reproduce the strongest cross-equatorial low level Somali Jet in the region 37.5°–62.5°E, and the stronger cross-equatorial low level flow in the region 100°–160°E with smaller cores than those of NCEP/NCAR reanalysis (Figs.1a,b). The simulated Somali Jet turns into northerly flow at upper levels. The simulated wind at 850 hPa in Fig.1c shows that southerly flow dominates over the Somali region, the easterlies prevail at 20°S and the westerlies control the Arabian Sea, Indian Peninsula, Bay of Bengal as well as South China Sea. In the difference of the 850-hPa wind field between the multi-model ensemble and the NCEP data (Fig.1d), there is a cyclonic anomaly to the south of the Arabian Sea, and there is an anticyclonic anomaly to the south of the Bay of Bengal. The multi-model ensemble can well describe circulations at 200 hPa including cross-equatorial northerly wind, the anticyclonic circulation of South Asian high as well as the tropical easterly jet (Fig.1e), where the simulated intensity of both the tropical easterly Jet and the upper level Somali Jet are weaker than those of NCEP/NCAR reanalysis (Fig.1f).

We define the index of intensity of Somali Jet as the area mean wind speed at 850 hPa in JJA in 15°S–10°N, 37.5°–62.5°E. The simulated (observed) average intensity of Somali Jet for the period 1976–1999 is 9.05 (9.5) m s^{-1}, the simulated (observed) interannual standard deviation is 0.12 (0.37) m s^{-1}. The multi-model ensemble therefore simulates a weaker Somali Jet than that in NCEP/NCAR data for 1976–1999. In addition, the standard deviation of 18 models at 0.71 m s^{-1} represents large differences among models.

3.3 Future changes of Somali Jet

We now analyze the future changes of Somali Jet during 2005–2099. The curve of 11-yr running mean intensity index of Somali Jet illustrates a weak period

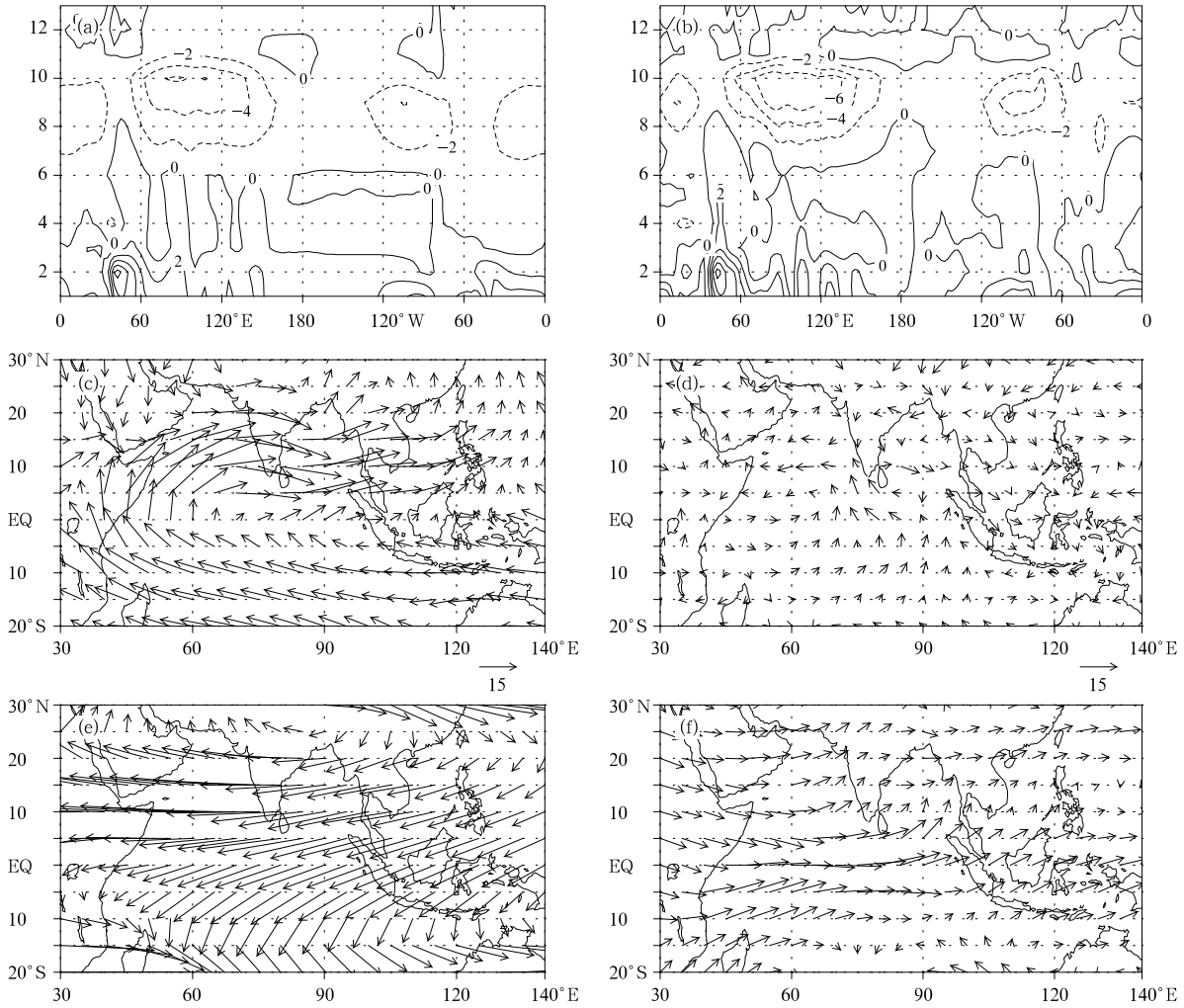

Fig.1. The longitude-altitude cross-sections of the meridional wind in summer along the equator. y axis from 1 to 13 represents 1000, 850, 700, 600, 500, 400, 300, 250, 200, 150, 100, 50, and 30 hPa, respectively, derived from (a) the multi-model ensemble and (b) NCEP/NCAR reanalysis; (c) 850-hPa wind field of the 18-model (20C3M) ensemble mean; (d) difference of the 850-hPa wind field between the 18-model (20C3M) ensemble mean and NCEP/NCAR reanalysis; (e) as in Fig.1c, but for 200 hPa; (f) as in Fig.1d, but for 200 hPa (unit: m s^{-1}).

in the early 21st century (2010–2040), an enhanced and strongest period during the middle 21st century (2050–2060), and a weakest period at the end of the 21st century (2070–2099). The 10-yr averaged intensity of Somali Jet is given in Table 2 for 2011–2099. Relative to the averaged intensity of Somali Jet (9.0 m s^{-1}) for the whole period 2005–2099, larger values occur during 2011–2020 and 2021–2030 while a smaller value occurs during 2031–2040, and the value is above normal for the period 2051–2060, which is the strongest in the whole period. Lower values appear during 2061–2070 and 2071–2080, and the lowest value during 2081–2090. Under the global warming, Somali Jet will become the strongest in the middle 21st century and the weakest at the end of the 21st century. In addition, compared to the period 1976–1999 (NCEP/NCAR, Fig.2b), the average value of SRESA2 (NCEP/NCAR) is 8.9 (9.5) m s^{-1}, Somali Jet will become obviously weaker in the future. Compared to the period 1976–1999 (20C3M), the increments of Somali Jet in every 10 yr for 2011–2099 are analyzed (Table 2). It is shown that the increment during 2051–2060

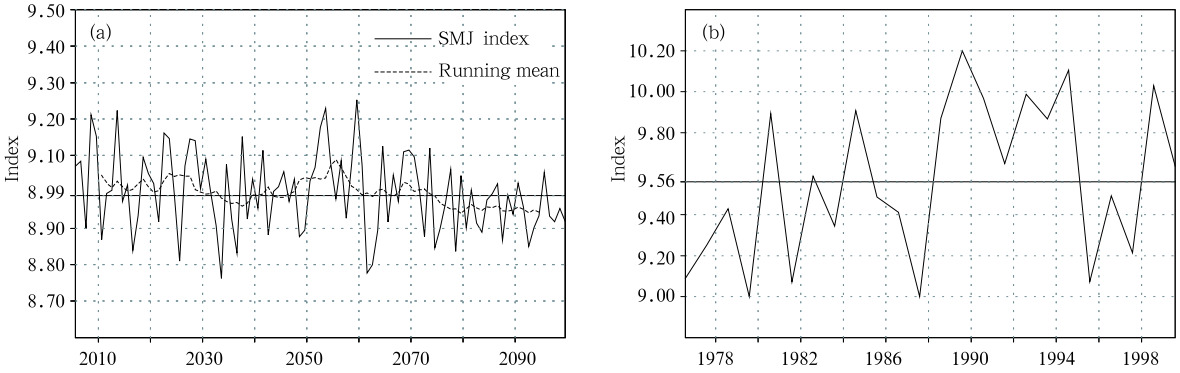

Fig.2. (a) Time series of the Somali Jet index (unit: m s^{-1}) during 2005–2099 with a 11-yr running mean. The thick solid line represents the average value for the period 2005–2099; (b) time series of the Somali Jet index (NCEP data) during 1976–1999. The thick solid line represents the average value for the period 1976–1999.

Table 2. The SRESA2 multi-model ensemble 10 yr mean intensity of Somali Jet (unit: m s^{-1}) for the period 2011–2099 and its difference relative to the mean value for 1976–1999 (20C3M)

	2011	2021	2031	2041	2051	2061	2071	2081	2091
A2	9.01	9.04	8.95	8.98	9.09	8.98	8.95	8.96	8.93
A2-20C3M	−0.03	−0.00	−0.09	−0.06	0.04	−0.06	−0.09	−0.08	−0.11

2011 and 2091 denote the period 2011–2020 and 2091–2099, respectively.

is positive, the other 10-yr increments are all negative, and the lowest value (−0.11 m s^{-1}) appears during 2091–2099, which means the magnitude of the largest increment is comparable to one standard variation (0.10 m s^{-1}) of the multi-model ensemble in SRESA2. In general, the intensity of Somali Jet would tend to become weaker in the future climate, specifically, it would be close to that of the present climate in the middle 21st century, and be the weakest at the end of the 21st century.

Figure 3 shows the wind difference between the period 2091–2099 and 1976–1999. Shaded areas indicate that the differences in the two meridional wind fields are statistically significant at 99% level. A *t*-test is performed using results from the 18 models to obtain the significant level. At 850 hPa, the wind difference between SRESA2 and 20C3M multi-model ensemble (Fig.3b) shows that the northerly anomaly dominates the Somali region, representing a weaker Somali Jet, accompanied by the occurrence of a westerly anomaly at 20°S related to the weaker Mascarene high, an easterly anomaly over 5°–10°N, and an anticyclonic anomaly around South Asia, the South China Sea, and western Pacific. These circulation changes associated with Somali Jet in summer are consistent with previous results, implying that weaker Somali Jet would result in a decrease of water vapor transport from the Southern Hemisphere to the Northern Hemisphere and would correspond to a weaker South China Sea monsoon and enhanced East Asian subtropical monsoon. By contrast, the southerly anomaly is remarkable in the Somali area along with a weaker South Asian high and a weaker tropical easterly jet at 200 hPa (Fig.3b). The circulation changes above indicate that the subtropical and tropical circulation systems will vary with Somali Jet in the future climate change. However, their inherent connection is complex and needs to be further explored.

3.4 Linkages between Somali Jet and global mean indent surface air temperature

What is the relationship between the intensity change of Somali Jet and the increase of global mean surface air temperature (GMSAT)? Would Somali Jet become weaker and weaker when the GMSAT increases in the future? How does Somali Jet variation

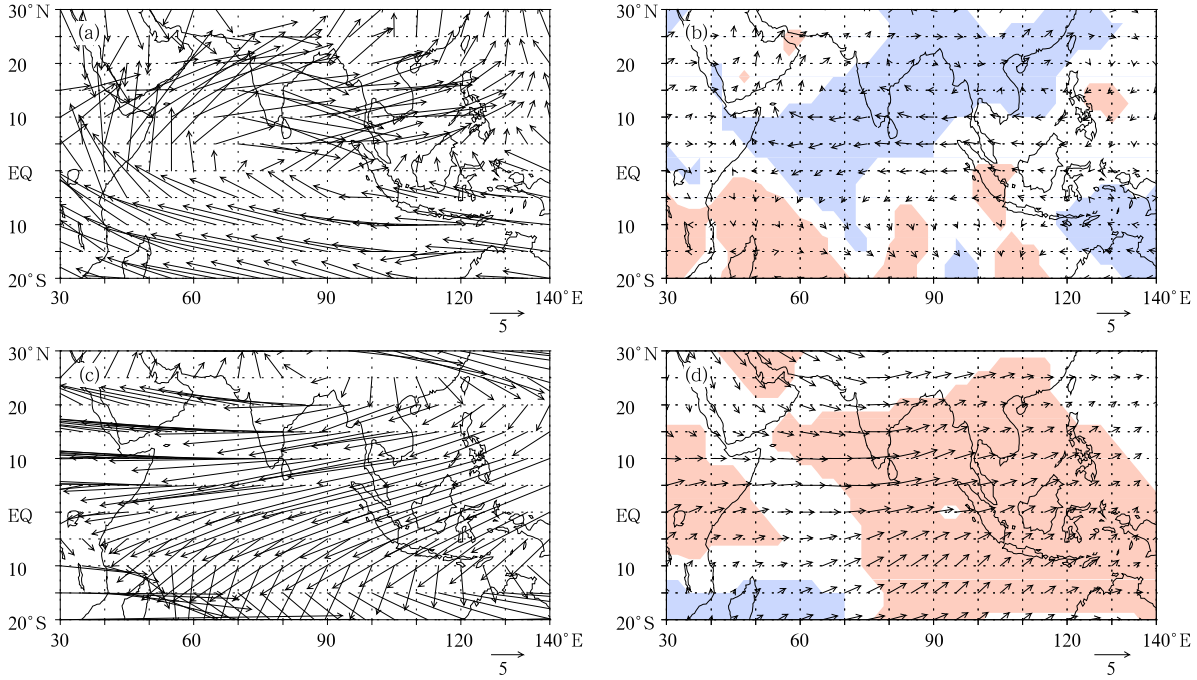

Fig.3. The SRESA2 multi-model ensemble wind and the wind difference between the SRESA2 multi-model ensemble (2091–2099) and 20C3M multi-model ensemble (1976–1999). (a) 850-hPa wind, (b) 850-hPa wind difference, (c) 200-hPa wind, and (d) 200-hPa wind difference. Shaded areas indicate the differences in meridional wind fields are statistically significant at 99% level (unit: m s^{-1}). t-test is performed using results from the 18 models to obtain the significant level.

rely on the increments of GMSAT? We divide the period 2011–2099 into 9 periods including 2011–2020, 2021–2030, 2031–2040, 2041–2050, 2051–2060, 2061–2070, 2071–2080, 2081–2090, and 2091–2099. The definition of the increment of GMSAT of each period is given here. For example, the increment of GMSAT for the period 2011–2020 is defined as the 10-yr (2011–2020) averaged SRESA2 multi-model ensemble GMSAT minus the 24-yr (1976–1999) averaged NCEP/NCAR reanalysis GMSAT. We use the increment of GMSAT in each 10-yr period as the x axis, and use the Somali Jet index in the same period in SRESA2 as the y axis, and then we obtain 9 dots. The relationship between the SRESA2 multi-model ensemble (each single model) Somali Jet intensity and the increment of GMSAT in 9 periods are depicted in Fig.4a (Fig.4b). Nine dots in every curve from the left to the right denote periods 2011–2020, 2021–2030, 2031–2040, 2041–2050, 2051–2060, 2061–2070, 2071–2080, 2081–2090, and 2091–2099, respectively.

When the increment of GMSAT is less than 1°C, Somali Jet will be weak. Somali Jet will be the strongest when the increment of GMSAT goes up to 1.5°C. Somali Jet will tend to weaken gradually when the increment of GMSAT is up to 2–3°C. Somali Jet will be the weakest when the increment of GMSAT is up to 3°C. However, the 18 models differ largely in the description of Somali Jet with the increasing GMSAT. Most models show that Somali Jet will fluctuate and then decrease, such as models A, E, H, N, O, and Q. Results from models C and L show that Somali Jet will weaken; models B, F, J, P, and R reflect the intensification of Somali Jet; models D, G, I, K, and M exhibit that Somali Jet will fluctuate. Figure 4 suggests that the relationship between Somali Jet changes and the increment of GMSAT is so complex and nonlinear that the strongest (weakest) Somali Jet does not correspond to the largest (smallest) increment of GMSAT. Each model describes the response of Somali Jet intensity to the increment of GMSAT differently.

Climate models, the mathematical expressions of the climate systems and reasonable physics,

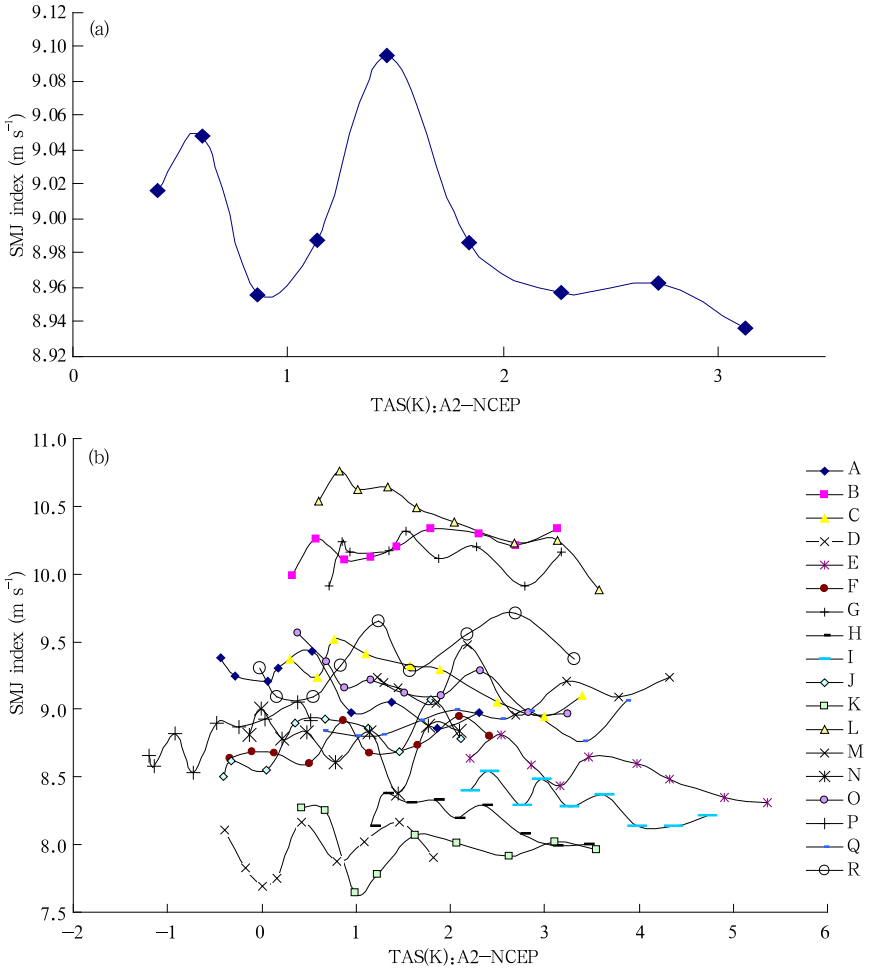

Fig.4. Time series of the 10-yr average intensity of Somali Jet during 2011–2099 and the corresponding increment of GMSAT (see the first paragraph of Section 3.4 for the increment definition) from (a) multi-model ensemble and (b) every single model. Nine points in every curve from the left to the right denote the period 2011–2020, 2021–2030, 2031–2040, 2041–2050, 2051–2060, 2061–2070, 2071–2080, 2081–2090, and 2091–2099. x axis is the increment of GMSAT, and y axis is the Somali Jet index.

are capable of reconstructing the climate changes in the present and future. However, our understanding of the climate systems is limited, and the mathematical frameworks of the climate systems cannot contain all the processes. In addition, various climate models describe the climate systems in different mathematical frameworks and use different physical parameters. Furthermore, the greenhouse gases concentration in SRESA2 is hypothetical. These factors will lead to the model inconsistency with the truth, and will increase the model uncertainties in projecting the future climate changes (For discussion about model uncertainties, please refer to Chapters 1, 8, 10, and 11 of the IPCC AR4 Working Group I Report, at the website: http://www.ipcc.ch/ipccreports/ar4-wg1.htm).

The standard deviation of the Somali Jet index for each 10-yr period as simulated by the 18 models of SRESA2 is analyzed in Table 3. It is found that the uncertainties of the Somali Jet index in each 10-yr mean do not change significantly, since the standard deviation of the Somali Jet index remains to be 0.70 m s^{-1} throughout the whole period 2011–2099. However, the model uncertainties in GMSAT are different. The 10-yr mean standard deviation of GMSAT increases

Table 3. Standard deviation (A2std) of the 10-yr mean intensity of Somali Jet (m s^{-1}) from the 18 models of SRESA2 and the increasing magnitude (K) (TASstd) of GMSAT for the period 2011–2099

	2011	2021	2031	2041	2051	2061	2071	2081	2091
A2std	0.68	0.74	0.79	0.77	0.73	0.71	0.75	0.69	0.70
TASstd	0.89	0.92	0.93	0.96	0.96	1.00	1.02	1.07	1.13

2011 and 2091 denote the period 2011–2020 and 2091–2099.

from 0.68°C to 1.13°C in the period of 2011–2099, which means the uncertainties of GMSAT simulated by various models increase with time.

4. Conclusions

Based on the outputs from 18 IPCC-AR4 ocean-atmosphere general models for the present climate simulations (20C3M) and for the future climate simulations (SRESA2), and through comparison with the NCEP/NCAR reanalysis and ERA-40 data, this investigation concludes that each of the 18 models and the multi-model ensemble are able to reproduce the observational features of Somali Jet and the associated circulation for the period 1976–1999. Further analysis of the Somali Jet future changes for the period 2005–2099 suggests that Somali Jet would decrease in the early 21st century and enhance in the middle 21st century, and then weaken at the end of the 21st century. Compared with the period 1976–1999, Somali Jet would weaken overall and be the weakest at the end of the 21st century.

There is a complex and nonlinear relationship between the Somali Jet changes and the increase of GMSAT. There is a large discrepancy among models in the description of the variability of Somali Jet and the increment of GMSAT of the same period. It is indicated that the response of Somali Jet intensity to the increment of GMSAT is such that the strongest (weakest) Somali Jet does not correspond to the largest (smallest) increment of GMSAT for all models. However, the multi-model ensemble outputs could reflect reasonably the common features of most models. The multi-model ensemble shows Somali Jet will be the strongest when the GMSAT increases by 1.5°C in the future. Subsequently, Somali Jet will be weakened to the lowest when the GMSAT increases by 3°C. In the future, it is important to study the relationship between Somali Jet and the GMSAT, also the mechanism for the influence of the global warming on Somali Jet.

The intensity changes of Somali Jet are closely associated with the variability of the South Asian monsoon, East Asian monsoon, and summer rainfall over eastern China. Actually, the complex variability of the East Asian and South Asian monsoon has shown significantly during the past 50 years. Therefore, future investigations on the relationship between Somali Jet and the Asian monsoon systems should be carried out in order to understand their variability and evolution in the future climate changes.

REFERENCES

Cong Jing, Guan Zhaoyong, and Wang Lijuan, 2007: Interannual (Interdecadal) variabilities of two cross-equatorial flows in association with the Asian summer monsoon variations. *Journal of Nanjing Institute of Meteorology*, **30**(6), 780–785. (in Chinese)

Gao Hui and Xue Feng, 2006: Seasonal variation of the cross-equatorial flows and their influences on the onset of South China Sea summer monsoon. *Climatic and Environmental Research*, **11**(1), 57–68. (in Chinese)

Gao Xuejie, Zhao Zongci, Ding Yihui, et al., 2003: Climate change due to greenhouse effects in China as simulated by a regional climate model. Part II: Climate change. *Acta Meteor. Sinica*, **61**(1), 29–38. (in Chinese)

Hegerl, G., G. Meehl, C. Covery, M. Latif, B. McAvaney, and R. Stouffer, 2003: 20C3M: CMIP collecting data from 20th century coupled model simulations. *CLIVAR exchange*, NO.26.

Hori, M. E., and H. Ueda, 2006: Impact of global warming on the East Asian winter monsoon as revealed by nine coupled atmosphere-ocean GCMS. *Geophys. Res. Lett.*, **33**(3), L03713, doi: 10.1029/2005GL024961.

Jiang Dabang, Wang Hunjun, and Lang Xianmei, 2004: Multimodel ensemble prediction for climate change

trend of China under SRES A2 scenario. *Chinese Journal of Geophysics*, **47**(5), 776–784.

Jiang Zhihong, Zhang Xia, and Wang Ji, 2008: Projection of climate change in China in the 21st century by IPCC-AR4 models. *Geographical Research*, **27**(4), 787–798. (in Chinese)

Li Xianghong, Xu Haiming, and He Jinhai, 2004: The study on the relationship between the west cross-equatorial flow and the heavy rain in South China. *Scientia Meteor. Sinica*, **24**(2), 161–167. (in Chinese)

Li Xiaofeng, Guo Pinwen, Dong Lina, et al., 2006: Onset process of summer Somali Jet and the possible influenced mechanism. *Journal of Nanjing Institute of Meteorology*, **29**(5), 601–605. (in Chinese)

Li Zengzhong and Lou Guangping, 1987: A study on the passages of cross-equatorial current during the southern monsoon. *Atmos. Sci.*, **11**(3), 313–319. (in Chinese)

Li Zengzhong, Qian Chanhai, and Sun Churong, 2000: A priliminary analysis on the relationship between the cross-equatorial flow and the heavy rainfall over Yangtze and Huanghe River in 1991. *Acta Meteor. Sinica*, **58**(5), 628–636. (in Chinese)

Shi Ning, Shi Danping, and Yan Mingliang, 2001: The effects of cross-equatorial current on South China Sea monsoon onset and drought/flood in East China. *Journal of Tropical Meteorology*, **17**(4), 405–415. (in Chinese)

Vera, C., G. Silvestri, B. Liebmann, et al., 2006: Climate change scenarios for seasonal precipitation in South America from IPCC-AR4 models. *Geophys. Res. Lett.*, **33**(13), L13707, doi: 10.1029/2005GL025759.

Wang Huijun and Xue Feng, 2003: Interannual variability of Somali Jet and its influences on the inter-hemispheric water vapor transport and on the East Asian summer rainfall. *Chinese Journal of Geophysics*, **46**(1), 18–25. (in Chinese)

Wang Huijun, Zeng Qingcun, and Zhang Xuehong, 1992: Numerical simulation of climate change induced by doubling CO_2 concentration. *Science in China (Ser.B)*, **22**(6), 663–672. (in Chinese)

Wang Weiping and Yang Xiuqun, 2008: Variation of Somali Jet and its impact on East Asian summer monsoon and associated China rainfall anomalies. *Scientia Meteor. Sinica*, **28**(2), 139–146. (in Chinese)

Xu Chonghai, Shen Xinyong, and Xu Ying, 2007: An analysis of climate change in East Asia by using the IPCC AR4 simulations. *Advances in Climate Change Research*, **3**(5), 287–292. (in Chinese)

Zhao Zongci and Luo Yong, 1998: Advance on investigations of regional climate modeling since 1990. *Acta Meteor. Sinica*, **56**(2), 225–246. (in Chinese)

Zhou Tianjun and Yu Rucong, 2006: 20th century surface air temperature over China and the globe simulated by coupled climate models. *J. Climate,* **19**(22), 5843–5858.